

POVQA: Preference-Optimized Video Question Answering with Rationales for Data Efficiency

Ashim Dahal Ankit Ghimire Saydul Akbar Murad Nick Rahimi
 University of Southern Mississippi
 Hattiesburg, Mississippi, USA

{ashim.dahal, ankit.ghimire, saydulakbar.murad, nick.rahimi}@usm.edu

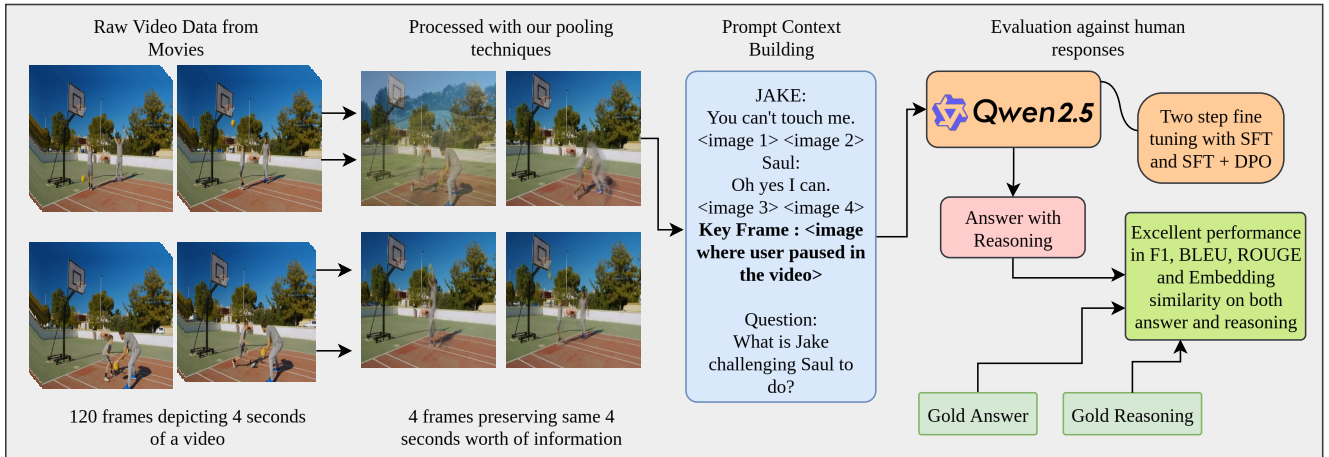


Figure 1. Overview of POVQA inference on the ReasonVQA evaluation split.

Abstract

Long-video multimodal question answering requires structured reasoning over visual evidence and dialogue, but Large Vision-Language Models (LVLMs) are constrained by context-window and compute limits. We propose POVQA, which compresses each second into a temporally pooled image (1 fps pooled images) to keep dense temporal coverage under a fixed token budget. We then train Qwen2.5-VL-7B with supervised fine-tuning (SFT) on rationale+answer targets (explicit chain-of-thought style supervision), and optionally apply Direct Preference Optimization (DPO) for preference alignment. We introduce ReasonVQA as a pilot diagnostic dataset with 12 movies and 239 human-annotated QA+rationale triplets for controlled analysis of long-context multimodal reasoning under compression. On ReasonVQA, SFT improves pooled baselines from 0.212 to 0.543 F1, 0.031 to 0.291 BLEU-4, and 0.196 to 0.528 ROUGE-L; zero-shot transfer on TVQA reaches 64.7% with SFT+DPO (and 69.7% for pooling-only inference). These results are preliminary: ReasonVQA is small, pooling can lose fine-grained temporal order, and DPO ef-

fects are not uniformly positive across settings.

1. Introduction

Video question answering (VQA) over movies and TV episodes requires combining dialogue, scene context, and temporally distributed visual evidence [17, 32]. This is a multimodal algorithmic reasoning setting: the model must integrate language and vision across time, then produce a structured answer grounded in evidence. In practice, long-video VQA remains difficult for modern Large Vision-Language Models (LVLMs): even large context windows represent only a short clip at native frame rates, while compute and memory grow quickly with video length [3, 7, 22, 24, 28, 30, 44].

A multi-minute clip contains thousands of frames. Feeding all frames is often infeasible, but aggressive frame dropping can remove key evidence for causal or temporal questions. This creates a core tradeoff between temporal coverage and token budget.

We study a simple long-context pipeline, POVQA, that

compresses video into 1 fps pooled images. Instead of selecting a few isolated frames, each pooled image summarizes a full second using blend-blur and weighted averaging variants. We then interleave pooled images with subtitle text and prompt an LVLM to generate both a rationale and a final answer, following the broader multimodal interleaving direction in prior works [14, 18, 33].

Pooling acts as a temporal evidence accumulator: each token encodes changes across many raw frames while keeping a fixed input length. This can preserve broad motion and scene transitions under a constrained budget, though it may fail on order-sensitive micro-actions. In this sense, POVQA targets test-time reasoning efficiency rather than architecture scaling.

We train with supervised fine-tuning (SFT) on rationale+answer outputs, then optionally apply Direct Preference Optimization (DPO). Rationale supervision encourages explicit evidence use, while DPO can align output style toward preferred responses in some regimes.

We use Qwen2.5-VL-7B for open weights, a strong vision-language backbone, and reproducible tooling. We do not claim this is the most efficient model; our focus is the input-compression and alignment recipe, which can later be tested on smaller backbones.

Contributions.

- A long-context multimodal reasoning pipeline that compresses long videos into a fixed-budget sequence of temporally pooled evidence images at 1 fps.
- A rationale-supervised SFT setup and a DPO variant, with analysis of where DPO helps or hurts in a small-data setting.
- ReasonVQA: a small pilot diagnostic dataset (12 movies, 239 QA+rationale triplets) for controlled evaluation of long-video reasoning under compression, including explicit failure-mode analysis.

Scope and limitations. This work is intentionally scoped as a pilot study, not a large benchmark release. ReasonVQA is small and movie-centric, pooling can miss fine-grained temporal order, and DPO can be unstable under limited preference data. We therefore position results as controlled evidence for this design choice rather than broad claims of generalization.

2. Related Work

2.1. Long-video understanding and benchmarks

Video question answering (VQA) benchmarks such as TVQA and MovieQA emphasize multi-step temporal reasoning across long narrative content [15, 17, 32]. Newer datasets (e.g., NExT-QA, STAR, AGQA, AVSD) further stress compositional and temporal understanding [2, 12, 40, 42]. Works such as KnowIT VQA and retrieval-augmented approaches further highlight dialogue and

external-knowledge dependencies [11, 13]. These benchmarks show that long-range evidence integration remains a bottleneck.

2.2. Video-LVLMs and multimodal instruction tuning

Recent LVLMs and video-language systems, including Flamingo, PaLI, Qwen-VL variants, Video-LLaVA, TimeChat, and MovieChat, improve general multimodal reasoning [3, 7, 22, 24, 28, 30, 44]. Stronger baselines such as LLaVA-Video and Video-LLaMA families are important comparison points for future large-scale evaluation. In this work we use Qwen2.5-VL-7B because it is open-weight, reproducible, and strong enough to test compression and supervision choices.

2.3. Temporal modeling, frame sampling, and pooling

Prior work studies keyframe selection, hierarchical grouping, memory modules, and efficient transformers to reduce video tokens [4, 9, 26, 29, 35, 39, 41, 45, 46]. Pooling and sampling approaches show that token budget is central to long-video performance, but can lose fine-grained timing signals when compression is too aggressive.

2.4. Preference optimization and alignment

Preference-based alignment methods such as DPO have been effective in language and multimodal settings for shaping response behavior [27]. Rationale-structured reasoning approaches are also increasingly studied for interpretability [23, 31]. In small-data regimes, however, preference supervision can be noisy and sensitive to pair quality, motivating cautious interpretation.

2.5. Efficiency, test-time constraints, and diagnostics

Recent work increasingly emphasizes inference-time constraints, token efficiency, and systematic stress-testing of reasoning systems [26, 35]. Our scope is aligned with this direction: we study lightweight evidence compression plus rationale alignment under limited annotation, and evaluate with explicit failure-mode analysis rather than broad benchmark claims.

Unlike large-benchmark works, we target practical long-video VQA under strict context budgets: lightweight compression can cover more seconds, while rationale supervision can improve answer consistency in a controlled pilot setting. We therefore position this as a diagnostics-first study of multimodal algorithmic reasoning under resource constraints.

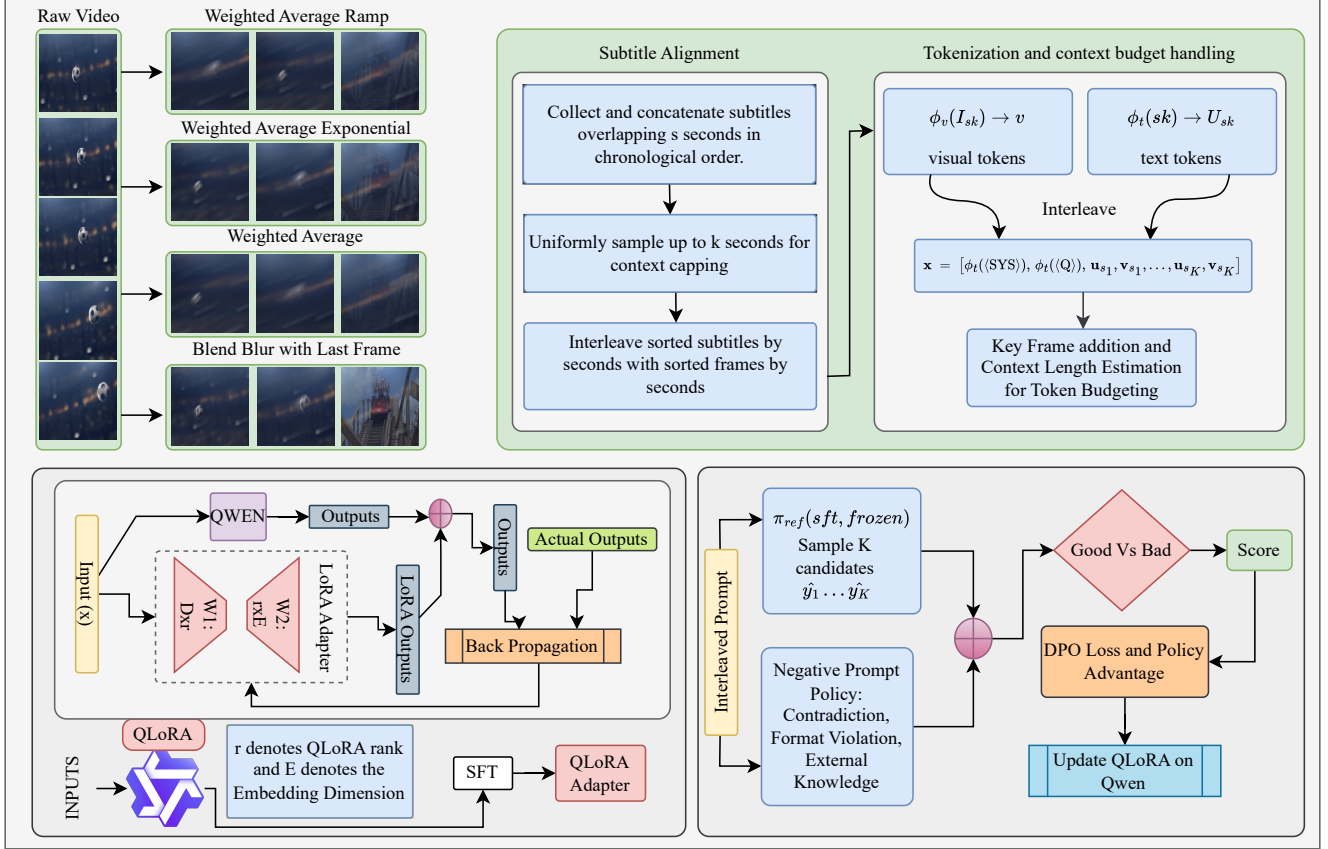


Figure 2. Overview of POVQA. (a) Video is compressed to 1 fps pooled images; (b) SFT trains rationale and final-answer generation; (c) optional DPO aligns preference pairs. Takeaway: temporal coverage is retained under a fixed token budget.

3. POVQA

POVQA takes a video and subtitle stream, pools raw frames into 1 fps pooled images, interleaves pooled images with subtitle text, and prompts an LVLm to generate a rationale and final answer. Training uses supervised fine-tuning (SFT) on rationale+answer targets, followed by optional Direct Preference Optimization (DPO). Evaluation reports lexical and embedding metrics on free-form outputs.

3.1. Notation

Let the video be $V = \{F_{t,k}\}$ where t indexes seconds and $k \in \{1, \dots, K\}$ indexes frames within second t . We denote the pooled image for second t as I_t , pooling weights as w_k with $\sum_{k=1}^K w_k = 1$, and the number of pooled visual tokens as T (approximately the video duration in seconds after truncation). Subtitle spans are $\mathcal{S} = \{(a_j, b_j, \text{text}_j)\}_{j=1}^J$.

For consistency with the equations below, we also use I_τ for the original frame sequence at f fps, where one-second windows define pooling groups:

$$W_s = \{I_\tau \mid \tau \in [(s-1)f + 1, sf]\}. \quad (1)$$

We denote the image encoder by $\phi_v(\cdot)$ (image \rightarrow visual tokens), the text tokenizer/embeddings by $\phi_t(\cdot)$, and the LVLm by $\pi_\theta(\cdot)$.

3.2. Temporal pooling and pooled frame construction

For each second s , choose nonnegative weights $w_s(\tau)$ on W_s with $\sum_{\tau \in W_s} w_s(\tau) = 1$, and form an average

$$\bar{I}_s = \sum_{\tau \in W_s} w_s(\tau) I_\tau. \quad (2)$$

Let $G_\sigma(\cdot)$ be a Gaussian blur and $I_s^{\text{last}} = I_{sf}$ the last frame in the second. We instantiate four operators:

Weighted Average (WA)

$$w_s(\tau) = \frac{1}{|W_s|}, \quad \tilde{I}_s = \bar{I}_s. \quad (3)$$

Weighted Average Exponential (WAE): recency bias

$$w_s(\tau) = \frac{\exp(\lambda(\tau - sf))}{\sum_{\kappa \in W_s} \exp(\lambda(\kappa - sf))}, \quad \lambda > 0, \quad \tilde{I}_s = \bar{I}_s. \quad (4)$$

Weighted Average Ramp (WAR): linear recency

$$w_s(\tau) = \frac{\tau - (s-1)f}{\sum_{\kappa \in W_s} (\kappa - (s-1)f)}, \quad \tilde{I}_s = \bar{I}_s. \quad (5)$$

Blend-Blur with Last Frame (BBLF)

$$\tilde{I}_s = \alpha I_s^{\text{last}} + (1-\alpha) G_\sigma(\bar{I}_s), \quad \alpha \in [0, 1], \sigma > 0. \quad (6)$$

Each \tilde{I}_s summarizes motion/appearance from 24–60 raw frames (depending on f), compressing intra-second dynamics into one image suitable for tokenization. This reduces visual sequence length from $O(\text{frames})$ to $O(\text{seconds})$.

Pooling keeps dense second-level coverage under a fixed context budget and can preserve broad “what changed” signals across scenes. The main failure mode is order-sensitive micro-actions (e.g., fast interactions or tiny objects), where second-level aggregation may blur or reorder crucial evidence.

3.3. Subtitle alignment and interleaving

Collect subtitles overlapping second s :

$$U_s = \bigoplus_{j: [a_j, b_j] \cap [(s-1), s] \neq \emptyset} \text{text}_j, \quad (7)$$

where \bigoplus concatenates spans in chronological order. Cap the context to S_{\max} seconds; if $S > S_{\max}$, uniformly subsample an index set

$$\mathcal{I} \subset \{1, \dots, S\}, \quad |\mathcal{I}| = K = \min(S, S_{\max}), \quad (8)$$

and sort $\{s_k\}_{k=1}^K = \text{sorted}(\mathcal{I})$. Build an interleaved sequence of subtitle spans and pooled images:

$$\mathcal{Z} = [U_{s_1}, \tilde{I}_{s_1}, U_{s_2}, \tilde{I}_{s_2}, \dots, U_{s_K}, \tilde{I}_{s_K}]. \quad (9)$$

3.4. Tokenization and model input

Map images and text to tokens:

$$\mathbf{v}_{s_k} = \phi_v(\tilde{I}_{s_k}) \in \mathbb{R}^{m \times d}, \quad \mathbf{u}_{s_k} = \phi_t(U_{s_k}), \quad (10)$$

and form the full input

$$\mathbf{x} = [\phi_t(\langle \text{SYS} \rangle), \phi_t(\langle \text{Q} \rangle), \mathbf{u}_{s_1}, \mathbf{v}_{s_1}, \dots, \mathbf{u}_{s_K}, \mathbf{v}_{s_K}]. \quad (11)$$

3.5. Prompting and rationale format

We elicit a rationale $\mathbf{y}^{(R)}$ (“Reasoning:”) and a short answer $\mathbf{y}^{(A)}$ (“Final Answer:”). The SYS prompt also includes 1 raw frame of the exact second the user paused the video in our player tool to ask question (if available). We call this frame as the key-frame of question.

We train the model to output rationale and answer in two fields: Reasoning: $\langle \text{grounded evidence} \rangle$ and Final Answer: $\langle \text{short answer} \rangle$. Rationales are explicit supervised targets during SFT and are part of preference pairs for DPO. Final-answer metrics (F1/BLEU/ROUGE) are computed on the Final Answer field; rationale similarity metrics are reported separately.

3.6. Supervised fine-tuning (SFT) with QLoRA

Given supervision $\mathbf{y} = [\mathbf{y}^{(R)}, \mathbf{y}^{(A)}]$, the SFT loss is

$$\mathcal{L}_{\text{SFT}}(\theta) = -\mathbb{E}_{(\mathbf{x}, \mathbf{y})} \sum_{i=1}^{|\mathbf{y}|} \log \pi_\theta(y_i | \mathbf{x}, \mathbf{y}_{<i}). \quad (12)$$

We implement SFT with QLoRA adapters for parameter-efficient tuning under limited hardware [10]. For a pre-trained matrix $W \in \mathbb{R}^{d_{\text{out}} \times d_{\text{in}}}$, QLoRA keeps a quantized frozen copy $q(W)$ and learns a low-rank update:

$$\begin{aligned} \Delta W &= \frac{\alpha}{r} BA, \\ A &\in \mathbb{R}^{r \times d_{\text{in}}}, \\ B &\in \mathbb{R}^{d_{\text{out}} \times r}, \\ r &\ll \min(d_{\text{in}}, d_{\text{out}}). \end{aligned} \quad (13)$$

Only A, B (and selected norms/biases) are trained under Eq. (12).

3.7. Direct Preference Optimization (DPO)

Let $\mathcal{D}_{\text{pref}} = \{(\mathbf{x}, \mathbf{y}^+, \mathbf{y}^-)\}$ be preference triples (preferred vs. dispreferred rationale+answer). With a frozen reference policy π_{ref} (the SFT model) and current policy π_θ , DPO minimizes

$$\begin{aligned} \Delta(\mathbf{x}, \mathbf{y}^+, \mathbf{y}^-) &= [\log \pi_\theta(\mathbf{y}^+ | \mathbf{x}) - \log \pi_\theta(\mathbf{y}^- | \mathbf{x})] \\ &\quad - [\log \pi_{\text{ref}}(\mathbf{y}^+ | \mathbf{x}) - \log \pi_{\text{ref}}(\mathbf{y}^- | \mathbf{x})]. \end{aligned} \quad (14)$$

where $\beta > 0$ and $\sigma(\cdot)$ is the logistic sigmoid. Sequence log-likelihoods expand tokenwise:

$$\log \pi_\theta(\mathbf{y} | \mathbf{x}) = \sum_{i=1}^{|\mathbf{y}|} \log \pi_\theta(y_i | \mathbf{x}, \mathbf{y}_{<i}). \quad (15)$$

Given Eq. (14), DPO minimizes the logistic loss

$$\mathcal{L}_{\text{DPO}}(\theta) = -\mathbb{E}_{(\mathbf{x}, \mathbf{y}^+, \mathbf{y}^-)} [\log \sigma(\beta \Delta(\mathbf{x}, \mathbf{y}^+, \mathbf{y}^-))] \quad (16)$$

where $\sigma(\cdot)$ is the logistic sigmoid and $\beta > 0$. In our setting, DPO is optional and analyzed cautiously: it can align responses toward preferred outputs, but small preference sets can introduce instability or metric tradeoffs.

3.8. Token budget and attention shift

Each pooled image yields m visual tokens and subtitles add $|\mathbf{u}_{s_k}|$ text tokens. For $K \leq S_{\max}$ seconds the context is

$$N_{\text{ctx}} \approx N_{\text{sys+Q}} + \sum_{k=1}^K (|\mathbf{u}_{s_k}| + m), \quad (17)$$

independent of raw fps f since pooling maps $\Theta(f)$ frames to m tokens/second. Thus motion is absorbed in \tilde{I}_s by ϕ_v ,

while temporal attention operates over adjacent pooled seconds. This design is related to prior work on segment-level temporal aggregation and video token efficiency [6, 34, 36].

For a 5-minute clip at 24 fps with $S_{\max} = 60$, $m = 256$, average subtitle length 10 tokens/second, and $N_{\text{sys}+Q} = 128$, pooled input is about 16,088 tokens versus about 369,368 tokens without pooling over the same 60-second budget. This is about a $23\times$ context reduction while preserving second-level temporal coverage.

3.9. Decoding

At inference we reuse Eq. (9)–Eq. (11) and decode sequentially with \mathcal{C} as the answer span regulator:

$$\hat{\mathbf{y}}^{(R)} = \arg \max_{\mathbf{y}} \pi_{\theta}(\mathbf{y} \mid \mathbf{x}, \text{“Reasoning:”}), \quad (18)$$

$$\hat{\mathbf{y}}^{(A)} = \arg \max_{\mathbf{y} \in \mathcal{C}} \pi_{\theta}(\mathbf{y} \mid \mathbf{x}, \hat{\mathbf{y}}^{(R)}, \text{“Final Answer:”}). \quad (19)$$

4. Experiments

4.1. Experimental Protocol

4.1.1. Dataset and splits

We use ReasonVQA, a pilot diagnostic dataset with 239 question–answer–rationale triplets from 12 movies (romance, historical, biography, western, fantasy, action, mystery, thriller, animation, drama, sci-fi, documentary). The evaluation split contains held-out sci-fi and western titles. Across all questions, the source context spans over 1M raw frames. This scale is intentionally small and is used for controlled ablation, not broad benchmark claims.

4.1.2. Input budget and decoding

Unless otherwise stated, we pool video to 1 fps pooled images, cap context to 60 pooled seconds, and interleave pooled images with subtitle text. For generation we decode rationale plus final answer with the same prompt format used in training.

4.1.3. Model and training

We adopt Qwen2.5-VL-7B for open weights and stable tooling. Our main hyperparameters are QLoRA rank/ $\alpha=32$, dropout=0.05, seed=42, grad-acc=8, learning rate $5e-5$ (SFT) and $5e-6$ (DPO). We append a key-frame instruction in the system prompt and uniformly sample 16 pooled frames per training step. Training used one NVIDIA A40-48Q (48 GB).

4.1.4. Baselines and fairness

We report three main settings: pooled-only (no fine-tuning), pooled+SFT, and pooled+SFT+DPO. We also include a keyframe-only ablation. For TVQA, our setting is zero-shot transfer from ReasonVQA; this is not directly comparable to fully supervised TVQA systems trained on TVQA labels.

Table 1. Transposed base results on ReasonVQA eval. B1/B4: BLEU-1/4, RL: ROUGE-L, EC: Embed Cos, RLR: ROUGE-L-R, ECR: Embed Cos-R. Highlights: highest, second-highest.

Metric	BBLF	WA	WAE	WAR	KF
F1	0.212	0.204	0.204	0.184	0.070
B1	0.453	0.441	0.405	0.380	0.159
B4	0.021	0.031	0.023	0.021	0.000
RL	0.196	0.187	0.183	0.168	0.069
EC	0.383	0.365	0.363	0.361	0.197
RLR	0.172	0.167	0.177	0.173	0.165
ECR	0.533	0.532	0.548	0.551	0.533

4.1.5. Metrics and their limitations

We report F1, BLEU, and ROUGE-L for final answers, plus embedding-similarity and overlap metrics for rationales. These metrics are useful for large ablations but do not perfectly track human judgment. We therefore include qualitative examples and a failure taxonomy. Unless noted, results are from single runs and variance is not reported. This evaluation protocol is intentionally diagnostic: we focus on systematic strengths and failure modes in multimodal reasoning under fixed test-time budgets.

4.2. Results

4.2.1. ReasonVQA

Table 1 reports pooled-only baselines before adaptation. Baseline answer quality is low (best F1 0.212). After two epochs of SFT, cross-evaluation results in Table 2 reach up to 0.550 F1 depending on train/eval pooling pairing; with SFT+DPO (Table 3), the best F1 is 0.543. Relative to pooled-only, SFT provides the main lift in this pilot setting. Rationale similarity also increases, e.g., Embed Cosine-R from 0.533 (base) to 0.597 (best DPO setting).

Table 4 shows that DPO effects are mixed: some rationale-oriented metrics improve, while answer-overlap metrics can be flat or slightly lower depending on the pooler. This is consistent with small-scale preference optimization, where pair noise and style alignment can trade off against lexical overlap.

This pattern matches DPO’s objective, which optimizes preference consistency rather than directly maximizing BLEU/ROUGE/F1. Overall, SFT drives most gains, while DPO is best interpreted as an optional alignment stage.

We can also observe from Tab. 3 and Tab. 2 that the diagonal is not always optimal. Under WAE evaluation, the best SFT model is cross-trained on BBLF (F1 = 0.533) rather than the diagonal (0.506). Under WAR evaluation, SFT’s best is the WA-trained model (F1 = 0.545) rather than the diagonal (0.526), whereas after DPO BBLF and WAE perform most consistently. This indicates that training on appearance-preserving pooling (BBLF) transfers well to

Table 2. Cross-evaluation of fine-tuned models after SFT in ReasonVQA eval set. Highlights: highest, second-highest, same training and evaluation method. Method abbreviations: BBLF (Blend Blur Last Frame), WA (Weighted Avg), WAE (Weighted Avg Exp), WAR (Weighted Avg Ramp), Metric-R (Metric- Reasoning)

Metric	Model Trained On			
	BBLF	WA	WAE	WAR
<i>Evaluated on: Blend Blur With Last Frame</i>				
F1	0.521	0.468	0.543	0.525
BLEU-1	0.574	0.520	0.603	0.581
BLEU-4 (BP)	0.245	0.209	0.265	0.257
ROUGE-L	0.499	0.445	0.520	0.504
Embed Cosine	0.620	0.573	0.632	0.617
ROUGE-L-R	0.227	0.206	0.227	0.225
Embed Cosine-R	0.586	0.583	0.590	0.587
<i>Evaluated on: Weighted Average</i>				
F1	0.521	0.523	0.550	0.535
BLEU-1	0.580	0.580	0.604	0.587
BLEU-4 (BP)	0.237	0.226	0.278	0.256
ROUGE-L	0.495	0.492	0.520	0.503
Embed Cosine	0.620	0.622	0.627	0.627
ROUGE-L-R	0.241	0.244	0.238	0.245
Embed Cosine-R	0.592	0.588	0.589	0.590
<i>Evaluated on: Weighted Average (Exp)</i>				
F1	0.533	0.520	0.506	0.520
BLEU-1	0.583	0.577	0.553	0.574
BLEU-4 (BP)	0.248	0.230	0.217	0.214
ROUGE-L	0.504	0.496	0.477	0.491
Embed Cosine	0.600	0.609	0.588	0.614
ROUGE-L-R	0.230	0.224	0.230	0.231
Embed Cosine-R	0.574	0.581	0.572	0.587
<i>Evaluated on: Weighted Average (Ramp)</i>				
F1	0.524	0.545	0.519	0.526
BLEU-1	0.575	0.603	0.572	0.586
BLEU-4 (BP)	0.224	0.247	0.216	0.228
ROUGE-L	0.490	0.512	0.488	0.495
Embed Cosine	0.622	0.630	0.605	0.620
ROUGE-L-R	0.236	0.243	0.242	0.241
Embed Cosine-R	0.597	0.596	0.596	0.592

motion-sensitive evaluation.

4.2.2. Zero-shot transfer to TVQA

We evaluate POVQA on the TVQA eval set in a strict zero-shot setting after fine tuning on ReasonVQA.

The only change to the pipeline in Fig. 2 is the system prompt to expose the answer options. We sample a random 5k subset for the evaluation split (scripts provided) for computational reason with $p \equiv 0.64$ and $n = 5000$ the normal approximated 95% CI is about ± 1.4 points.

Table 3. Cross-evaluation of fine-tuned models after SFT + DPO in ReasonVQA eval set. Highlights: highest, second-highest, same training and evaluation method. Method abbreviations: BBLF (Blend Blur Last Frame), WA (Weighted Avg), WAE (Weighted Avg Exp), WAR (Weighted Avg Ramp), Metric-R (Metric- Reasoning)

Metric	Model Trained On			
	BBLF	WA	WAE	WAR
<i>Evaluated on: Blend Blur With Last Frame</i>				
F1	0.505	0.506	0.541	0.495
BLEU-1	0.553	0.558	0.583	0.543
BLEU-4 (BP)	0.231	0.218	0.267	0.233
ROUGE-L	0.484	0.482	0.513	0.474
Embed Cosine	0.614	0.614	0.631	0.592
ROUGE-L-R	0.230	0.224	0.233	0.224
Embed Cosine-R	0.588	0.588	0.597	0.587
<i>Evaluated on: Weighted Average</i>				
F1	0.518	0.527	0.541	0.483
BLEU-1	0.573	0.580	0.594	0.531
BLEU-4 (BP)	0.254	0.246	0.272	0.217
ROUGE-L	0.496	0.501	0.518	0.459
Embed Cosine	0.605	0.619	0.610	0.575
ROUGE-L-R	0.228	0.236	0.229	0.227
Embed Cosine-R	0.585	0.586	0.586	0.587
<i>Evaluated on: Weighted Average (Exp)</i>				
F1	0.526	0.521	0.505	0.514
BLEU-1	0.568	0.575	0.560	0.562
BLEU-4 (BP)	0.240	0.226	0.212	0.210
ROUGE-L	0.498	0.498	0.479	0.489
Embed Cosine	0.602	0.608	0.577	0.599
ROUGE-L-R	0.234	0.231	0.226	0.229
Embed Cosine-R	0.587	0.592	0.574	0.586
<i>Evaluated on: Weighted Average (Ramp)</i>				
F1	0.543	0.535	0.512	0.541
BLEU-1	0.602	0.597	0.571	0.600
BLEU-4 (BP)	0.273	0.230	0.233	0.252
ROUGE-L	0.516	0.502	0.483	0.512
Embed Cosine	0.624	0.621	0.585	0.629
ROUGE-L-R	0.243	0.242	0.232	0.246
Embed Cosine-R	0.593	0.594	0.591	0.589

POVQA (SFT+DPO) attains 64.7% zero-shot accuracy on TVQA [17], while pooling-only attains 69.7% (Tabs. 5 and 7). Because many prior systems in Table 5 are trained under different supervision or modality settings, we treat this comparison as contextual rather than a like-for-like leaderboard claim.

Table 2 indicates that SFT consistently improves over pooled-only baselines and that cross-pooler transfer is often stronger than diagonal-only training.

Table 4. DPO vs. SFT deltas by evaluation pooler (best over training poolers) in ReasonVQA eval set. $\Delta = \text{DPO} - \text{SFT}$; positive means DPO helps. Highlights: highest, second-highest.

Metric	Model Trained On			
	BBLF	WA	WAE	WAR
F1	-0.002	-0.009	-0.007	-0.002
BLEU-1	-0.020	-0.010	-0.008	-0.001
BLEU-4 (BP)	+0.002	-0.006	-0.008	+0.026
ROUGE-L	-0.007	-0.002	-0.006	+0.004
Embed Cosine	-0.001	-0.008	-0.006	-0.001
ROUGE-L-R	+0.006	-0.009	+0.003	+0.003
Embed Cosine-R	+0.007	-0.005	+0.005	-0.003

Table 3 shows that DPO is competitive but not uniformly better than SFT-only on answer overlap, reinforcing cautious interpretation in small-data settings.

4.2.3. DPO analysis

From Table 4, DPO tends to help more on rationale-oriented metrics than on strict lexical answer metrics. A plausible explanation is preference-pair noise and overfitting in a limited corpus: for ambiguous questions, DPO can improve concise preference alignment, while for precise temporal ordering it can slightly reduce lexical match.

We highlight only the gap between pooling vs. keyframe under identical zero-shot protocol; other rows are for context.

4.3. Ablation

Most of our experiments were ablation-driven to isolate the effect of (i) frame-pooling strategy, (ii) supervision objective (SFT vs. DPO), and (iii) frame selection (retaining motion-blurred frames). Tab. 1 establishes the lower bound by removing motion-blurred frames and yields among the lowest scores, indicating that even “imperfect” frames contribute temporal evidence. Building on that, Tabs. 1 to 3 report the full cross-evaluation sweep across four pooling strategies: Blend BBLF, WA, WAE, and WAR under both SFT and DPO (37 configurations). Across these multi-frame sweeps, BBLF emerges as the most consistently strong choice after fine-tuning. To probe the strength of single-frame shortcuts against our 60-frame regime, we additionally ran a KeyFrame-only ablation (+8 configurations) and TVQA zero-shot runs bringing the total to 50 experimental sweeps.

Tab. 6 shows that KeyFrame-only token metrics cluster tightly (F1 0.553–0.563, ROUGE-L 0.518–0.528, BLEU-4 0.287–0.291), i.e., they are largely insensitive to temporal evidence. The only clearly positive deltas appear on embedding-based metrics: Embed Cosine $\Delta = +0.013$ and Embed Cos-R $\Delta = +0.033$, which capture semantic fidelity that a single frame cannot supply. In contrast, lexical deltas are near-zero or slightly negative (F1 -0.005 ,

Table 5. TVQA accuracy (%) for contextual reference; settings differ in supervision/modality. Zero-shot means no TVQA training. “w/ speech” = ASR/subtitles used. Our row reports the best across evaluation poolers (BBLF/WA/WAE/WAR) with training on BBLF only. Highlights: our result, selected reference results.

Model	Zero-shot	Venue (Year)	Acc.
FrozenBiLM [43]	✗	NeurIPS (2022)	82.0
VINDLU [8]	✗	CVPR (2023)	79.0
HERO [21]	✗	EMNLP (2020)	74.24
SeViLA [47]	✗	NeurIPS (2023)	61.6
ViLA [37]	✗	ECCV (2024)	63.4
BLIP-2 [19]	✗	ICML (2023)	54.5
InternVideo [38]	✗	arXiv (2022)	57.2
FrozenBiLM (w/ speech) [43]	✓	NeurIPS (2022)	59.7
FrozenBiLM (vision-only) [43]	✓	NeurIPS (2022)	29.7
IG-VLM (LLaVA-1.6 34B) [16]	✓	IEEE Access (2024)	51.1
GPT-4V (via IG-VLM) [1, 16]	✓	arXiv (2024)	57.8
Goldfish-7B (vision+subs) [5]	✓	ECCV (2024)	46.94
Goldfish-7B (vision only) [5]	✓	ECCV (2024)	36.45
Q-ViD [25]	✓	Findings ACL (2024)	41.0
VideoChat2 (reported by Q-ViD) [20]	✓	CVPR (2024)	40.6
SeViLA (reported by Q-ViD) [47]	✓	NeurIPS (2023)	38.2
InternVideo (reported by Q-ViD) [38]	✓	arXiv (2022)	35.9
POVQA (ours)	✓	This work (2026)	64.7

Table 6. KeyFrame-only ablation (max over SFT/DPO per method). highest, second-highest per row. $\Delta = \text{best DPO (over methods)} - \text{best KeyFrame ablation (over methods)}$.

Metric	BBLF	WA	WAE	WAR	Δ
F1	0.558	0.553	0.555	0.563	-0.005
BLEU-1	0.618	0.616	0.621	0.620	-0.003
BLEU-4 (BP)	0.289	0.287	0.291	0.291	+0.000
ROUGE-L	0.523	0.518	0.524	0.528	-0.007
Embed Cosine	0.619	0.616	0.602	0.617	+0.013
ROUGE-L-R	0.240	0.246	0.243	0.240	+0.000
Embed Cos-R	0.562	0.564	0.562	0.561	+0.033

BLEU-1 -0.003 , ROUGE-L -0.007). Thus, even when token scores look close under KeyFrame-only evaluation, using all 60 frames primarily buys semantic grounding and reasoning consistency, which is exactly what VQA is supposed to test.

4.4. Qualitative Analysis and Failure Cases

Figs. 3a and 3b show both successful and failure examples. Success cases typically involve broad scene context

Question: Why did Bob say he put a new transmission in Larry's truck when he was confessing to all of the people?



Show: House M.D. • Clip: house_s08e05_ssg02_clip_14 • Span: 2:15-37:41
 Pooling method: blend blur with last frame
 Subtitles: [No speech] (Bob)Larry, that new transmission I put in your truck, [No speech] (Bob)you didn't need it. [No speech]

Reasoning Analysis:

Human Reference

- He had cheated him.
- A Because he wanted his transmission to run like new.
 - B He really needed a new transmission.
 - C He had cheated him.
 - D Because he wanted to learn more about transmissions.
 - E Because his wife had insisted he do it.

Model Output

In this scene, Bob is confessing to everyone that he had been cheating on his wife. He had been having an affair with a woman who was a doctor. In the previous scene, he had told his wife that he had a new transmission installed in his truck. In this scene, he is confessing to everyone that he had been cheating on his wife by saying that he had installed a new transmission in her truck. This was a lie because he had not installed a new transmission at all. He had been having an affair with the woman who was a doctor and she had been the one who had installed the new transmission in his truck. So, he had cheated on his wife.

Model's Choice: C

(a) TVQA qualitative samples.

Question: How many people are in the screen at this particular timestep?



Pooling method: blend blur with last frame
 Subtitles: [No speech] Are you afraid, Ramon? [No speech] You shoot to kill, you better hit the heart. [No speech] Your own words, Ramon. [No speech] [No speech]

Reasoning Analysis:

Human Reference

In this timestep or frame two people's back can be seen. Another person can be seen putting his hands on the two barrels and the fourth person whose hands are hanging with a rope.

Model Output — blend blur with last frame

In this scene there is one person holding a gun and another person standing behind him. There is also a man who is hanging on a rope. In the background there are some other people standing around. So there are 4 people in total.

Answers:

Human Answer

There are 4 people in the screen at this particular timestep.

Model Output — blend blur with last frame

There are four people in the screen at this particular timestep

(b) ReasonVQA qualitative samples.

Figure 3. Qualitative analysis with on 2 randomly selected examples. Frames are sub-sampled for readability.

Table 7. TVQA base (no fine-tuning).

Setting	Accuracy
Pooling only	69.7%
KeyFrame only	56.8%

or character-state changes that are preserved by second-level pooling. Failure cases mainly follow four patterns: temporal-order errors in fast actions, small object/action misses, dialogue-dependency errors, and occlusion or hard scene cuts. These failure modes match the known limitations of temporal pooling under fixed context budgets.

On TVQA, the zero-shot base model with interleaved pooling surpasses our SFT/DPO adapters, whereas the KeyFrame-only variant lags (Tab. 7). This indicates that temporal pooling is a primary driver of transfer in our setup; preference tuning may require larger, domain-matched preference pairs to improve accuracy consistently.

We also present two random samples of the result produced by our model after SFT + DPO in Fig. 3a and Fig. 3b.

5. Conclusion

We presented POVQA for long-video multimodal reasoning under strict context budgets. The method compresses video into 1 fps pooled images, supervises rationale+answer generation with SFT, and optionally applies DPO for preference alignment. In our pilot setting, the main gain comes from pooled evidence plus SFT, while DPO is helpful in some regimes and neutral or negative in others.

ReasonVQA is a pilot diagnostic dataset (12 movies, 239 QA+rationale triplets) intended for controlled analysis rather than large-scale benchmarking. In this setting, we observe strong improvements over pooled-only baselines on answer and rationale metrics, non-trivial zero-shot transfer to TVQA, and interpretable failure patterns tied to temporal

compression. Overall, the study emphasizes test-time efficiency and transparent shortcomings analysis in multimodal reasoning.

Limitations. This study has several limitations: (i) small dataset scale and movie-domain bias, (ii) pooling can lose fine-grained temporal order and tiny action cues, (iii) DPO instability with limited preference pairs, and (iv) metric mismatch between lexical overlap and human-judged reasoning quality.

Future work. Future directions include expanding the dataset, evaluating on standard long-video benchmarks with stronger video-native baselines, adding judge-based or task-specific accuracy metrics, and testing the same compression recipe on smaller and larger backbones.

References

- [1] Josh Achiam, Steven Adler, Sandhini Agarwal, Lama Ahmad, Ilge Akkaya, Florencia Leoni Aleman, Diogo Almeida, Janko Altenschmidt, Sam Altman, Shyamal Anadkat, et al. Gpt-4 technical report. *arXiv preprint arXiv:2303.08774*, 2023. 7
- [2] Huda Alamri, Vincent Cartillier, Raphael Gontijo Lopes, Abhishek Das, Jue Wang, Irfan Essa, Dhruv Batra, Devi Parikh, Anoop Cherian, Tim K Marks, et al. Audio visual scene-aware dialog (avsd) challenge at dstc7. *arXiv preprint arXiv:1806.00525*, 2018. 2
- [3] Jean-Baptiste Alayrac, Jeff Donahue, Pauline Luc, Antoine Miech, Iain Barr, Yana Hasson, Karel Lenc, Arthur Mensch, Katherine Millican, Malcolm Reynolds, et al. Flamingo: a visual language model for few-shot learning. *Advances in neural information processing systems*, 35:23716–23736, 2022. 1, 2
- [4] Anurag Arnab, Mostafa Dehghani, Georg Heigold, Chen Sun, Mario Lučić, and Cordelia Schmid. Vivit: A video vision transformer. In *Proceedings of the IEEE/CVF international conference on computer vision*, pages 6836–6846, 2021. 2

- [5] Kirolos Ataallah, Xiaoqian Shen, Eslam Abdelrahman, Essam Sleiman, Mingchen Zhuge, Jian Ding, Deyao Zhu, Jürgen Schmidhuber, and Mohamed Elhoseiny. Goldfish: Vision-language understanding of arbitrarily long videos. In *European Conference on Computer Vision*, pages 251–267. Springer, 2024. 7
- [6] Gedas Bertasius, Heng Wang, and Lorenzo Torresani. Is space-time attention all you need for video understanding? In *Proceedings of the 38th International Conference on Machine Learning*, pages 813–824. PMLR, 2021. 5
- [7] Xi Chen, Josip Djolonga, Piotr Padlewski, Basil Mustafa, Soravit Changpinyo, Jialin Wu, Carlos Riquelme Ruiz, Sebastian Goodman, Xiao Wang, Yi Tay, et al. Pali-x: On scaling up a multilingual vision and language model. *arXiv preprint arXiv:2305.18565*, 2023. 1, 2
- [8] Feng Cheng, Xizi Wang, Jie Lei, David Crandall, Mohit Bansal, and Gedas Bertasius. Vindlu: A recipe for effective video-and-language pretraining. In *Proceedings of the IEEE/CVF Conference on Computer Vision and Pattern Recognition*, pages 10739–10750, 2023. 7
- [9] Zihang Dai, Zhilin Yang, Yiming Yang, Jaime Carbonell, Quoc V Le, and Ruslan Salakhutdinov. Transformer-xl: Attentive language models beyond a fixed-length context. *arXiv preprint arXiv:1901.02860*, 2019. 2
- [10] Tim Dettmers, Artidoro Pagnoni, Ari Holtzman, and Luke Zettlemoyer. Qlora: Efficient finetuning of quantized llms. *Advances in neural information processing systems*, 36: 10088–10115, 2023. 4
- [11] Noa Garcia, Mayu Otani, Chenhui Chu, and Yuta Nakashima. Knowit vqa: Answering knowledge-based questions about videos. In *Proceedings of the AAAI conference on artificial intelligence*, pages 10826–10834, 2020. 2
- [12] Madeleine Grunde-McLaughlin, Ranjay Krishna, and Maneesh Agrawala. Agqa 2.0: An updated benchmark for compositional spatio-temporal reasoning. *arXiv preprint arXiv:2204.06105*, 2022. 2
- [13] Ziniu Hu, Ahmet Iscen, Chen Sun, Zirui Wang, Kai-Wei Chang, Yizhou Sun, Cordelia Schmid, David A Ross, and Alireza Fathi. Reveal: Retrieval-augmented visual-language pre-training with multi-source multimodal knowledge memory. In *Proceedings of the IEEE/CVF conference on computer vision and pattern recognition*, pages 23369–23379, 2023. 2
- [14] Dongfu Jiang, Xuan He, Huaye Zeng, Cong Wei, Max W.F. Ku, Qian Liu, and Wenhui Chen. Mantis: Interleaved multi-image instruction tuning. *Trans. Mach. Learn. Res.*, 2024, 2024. 2
- [15] Kushal Kafle and Christopher Kanan. Visual question answering: Datasets, algorithms, and future challenges. *Computer Vision and Image Understanding*, 163:3–20, 2017. 2
- [16] Wonkyun Kim, Changin Choi, Wonseok Lee, and Wonjong Rhee. An image grid can be worth a video: Zero-shot video question answering using a vlm. *IEEE Access*, 2024. 7
- [17] Jie Lei, Licheng Yu, Mohit Bansal, and Tamara L Berg. Tvqa: Localized, compositional video question answering. *arXiv preprint arXiv:1809.01696*, 2018. 1, 2, 6
- [18] Feng Li, Renrui Zhang, Hao Zhang, Yuanhan Zhang, Bo Li, Wei Li, Zejun Ma, and Chunyuan Li. Llava-next-interleave: Tackling multi-image, video, and 3d in large multimodal models. *arXiv preprint arXiv:2407.07895*, 2024. 2
- [19] Junnan Li, Dongxu Li, Silvio Savarese, and Steven Hoi. Blip-2: Bootstrapping language-image pre-training with frozen image encoders and large language models. In *International conference on machine learning*, pages 19730–19742. PMLR, 2023. 7
- [20] Kunchang Li, Yali Wang, Yinan He, Yizhuo Li, Yi Wang, Yi Liu, Zun Wang, Jilan Xu, Guo Chen, Ping Luo, et al. Mvbench: A comprehensive multi-modal video understanding benchmark. In *Proceedings of the IEEE/CVF Conference on Computer Vision and Pattern Recognition*, pages 22195–22206, 2024. 7
- [21] Linjie Li, Yen-Chun Chen, Yu Cheng, Zhe Gan, Licheng Yu, and Jingjing Liu. HERO: Hierarchical encoder for Video+Language omni-representation pre-training. In *Proceedings of the 2020 Conference on Empirical Methods in Natural Language Processing (EMNLP)*, pages 2046–2065, Online, 2020. Association for Computational Linguistics. 7
- [22] Bin Lin, Bin Zhu, Yang Ye, Munan Ning, Peng Jin, and Li Yuan. Video-llava: Learning united visual representation by alignment before projection. *EMNLP*, 2023. 1, 2
- [23] Huabin Liu, Filip Ilievski, and Cees GM Snoek. Commonsense video question answering through video-grounded entailment tree reasoning. In *Proceedings of the Computer Vision and Pattern Recognition Conference*, pages 3262–3271, 2025. 2
- [24] Muhammad Maaz, Hanoona Rasheed, Salman Khan, and Fahad Shahbaz Khan. Video-chatgpt: Towards detailed video understanding via large vision and language models. In *Proceedings of the 62nd Annual Meeting of the Association for Computational Linguistics (ACL 2024)*, 2024. 1, 2
- [25] David Mogrovejo and Thamar Solorio. Question-instructed visual descriptions for zero-shot video answering. In *Findings of the Association for Computational Linguistics ACL 2024*, pages 9329–9339, 2024. 7
- [26] Rui Qian, Xiaoyi Dong, Pan Zhang, Yuhang Zang, Shuangrui Ding, Dahua Lin, and Jiaqi Wang. Streaming long video understanding with large language models. *Advances in Neural Information Processing Systems*, 37:119336–119360, 2024. 2
- [27] Rafael Rafailov, Archit Sharma, Eric Mitchell, Christopher D Manning, Stefano Ermon, and Chelsea Finn. Direct preference optimization: Your language model is secretly a reward model. *Advances in neural information processing systems*, 36:53728–53741, 2023. 2
- [28] Shuhuai Ren, Linli Yao, Shicheng Li, Xu Sun, and Lu Hou. Timechat: A time-sensitive multimodal large language model for long video understanding. In *Proceedings of the IEEE/CVF Conference on Computer Vision and Pattern Recognition*, pages 14313–14323, 2024. 1, 2
- [29] Shikhar Sharma, Ryan Kiros, and Ruslan Salakhutdinov. Action recognition using visual attention. *arXiv preprint arXiv:1511.04119*, 2015. 2
- [30] Enxin Song, Wenhao Chai, Guanhong Wang, Yucheng Zhang, Haoyang Zhou, Feiyang Wu, Haozhe Chi, Xun Guo, Tian Ye, Yanting Zhang, et al. Moviechat: From dense token

- to sparse memory for long video understanding. In *Proceedings of the IEEE/CVF Conference on Computer Vision and Pattern Recognition*, pages 18221–18232, 2024. 1, 2
- [31] Zihan Song, Xin Wang, Zi Qian, Hong Chen, Longtao Huang, Hui Xue, and Wenwu Zhu. Modularized self-reflected video reasoner for multimodal llm with application to video question answering. In *Forty-second International Conference on Machine Learning*. 2
- [32] Makarand Tapaswi, Yukun Zhu, Rainer Stiefelhagen, Antonio Torralba, Raquel Urtasun, and Sanja Fidler. Movieqa: Understanding stories in movies through question-answering. In *Proceedings of the IEEE conference on computer vision and pattern recognition*, pages 4631–4640, 2016. 1, 2
- [33] Changyao Tian, Xizhou Zhu, Yuwen Xiong, Weiyun Wang, Zhe Chen, Wenhai Wang, Yuntao Chen, Lewei Lu, Tong Lu, Jie Zhou, Hongsheng Li, Yu Qiao, and Jifeng Dai. Mm-interleaved: Interleaved image-text generative modeling via multi-modal feature synchronizer. *ArXiv*, abs/2401.10208, 2024. 2
- [34] Zhan Tong, Yibing Song, Jue Wang, and Limin Wang. Videomae: Masked autoencoders are data-efficient learners for self-supervised video pre-training. *Advances in neural information processing systems*, 35:10078–10093, 2022. 5
- [35] Pavan Kumar Anasosalu Vasu, Fartash Faghri, Chun-Liang Li, Cem Koc, Nate True, Albert Antony, Gokula Santhanam, James Gabriel, Peter Grasch, Oncel Tuzel, et al. Fastvlm: Efficient vision encoding for vision language models. In *Proceedings of the Computer Vision and Pattern Recognition Conference*, pages 19769–19780, 2025. 2
- [36] Limin Wang, Yuanjun Xiong, Zhe Wang, Yu Qiao, Dahua Lin, Xiaoou Tang, and Luc Van Gool. Temporal segment networks: Towards good practices for deep action recognition. *CoRR*, abs/1608.00859, 2016. 5
- [37] Xijun Wang, Junbang Liang, Chun-Kai Wang, Kenan Deng, Yu Lou, Ming C Lin, and Shan Yang. Vila: Efficient video-language alignment for video question answering. In *European Conference on Computer Vision*, pages 186–204. Springer, 2024. 7
- [38] Yi Wang, Kunchang Li, Yizhuo Li, Yanan He, Bingkun Huang, Zhiyu Zhao, Hongjie Zhang, Jilan Xu, Yi Liu, Zun Wang, et al. Internvideo: General video foundation models via generative and discriminative learning. *arXiv preprint arXiv:2212.03191*, 2022. 7
- [39] Yuetian Weng, Mingfei Han, Haoyu He, Xiaojun Chang, and Bohan Zhuang. Longvlm: Efficient long video understanding via large language models. In *European Conference on Computer Vision*, pages 453–470. Springer, 2024. 2
- [40] Bo Wu, Shoubin Yu, Zhenfang Chen, Joshua B Tenenbaum, and Chuang Gan. Star: A benchmark for situated reasoning in real-world videos. *arXiv preprint arXiv:2405.09711*, 2024. 2
- [41] Zuxuan Wu, Caiming Xiong, Chih-Yao Ma, Richard Socher, and Larry S Davis. Adaframe: Adaptive frame selection for fast video recognition. In *Proceedings of the IEEE/CVF Conference on Computer Vision and Pattern Recognition*, pages 1278–1287, 2019. 2
- [42] Junbin Xiao, Xindi Shang, Angela Yao, and Tat-Seng Chua. Next-qa: Next phase of question-answering to explaining temporal actions. In *Proceedings of the IEEE/CVF conference on computer vision and pattern recognition*, pages 9777–9786, 2021. 2
- [43] Antoine Yang, Antoine Miech, Josef Sivic, Ivan Laptev, and Cordelia Schmid. Zero-shot video question answering via frozen bidirectional language models. *Advances in Neural Information Processing Systems*, 35:124–141, 2022. 7
- [44] An Yang, Bowen Yu, Chengyuan Li, Dayiheng Liu, Fei Huang, Haoyan Huang, Jiandong Jiang, Jianhong Tu, Jianwei Zhang, Jingren Zhou, et al. Qwen2. 5-1m technical report. *arXiv preprint arXiv:2501.15383*, 2025. 1, 2
- [45] Xuyi Yang, Wenhao Zhang, Hongbo Jin, Lin Liu, Hongbo Xu, Yongwei Nie, Fei Yu, and Fei Ma. Enhancing long video question answering with scene-localized frame grouping. *arXiv preprint arXiv:2508.03009*, 2025. 2
- [46] Xuyi Yang, Wenhao Zhang, Hongbo Jin, Lin Liu, Hongbo Xu, Yongwei Nie, Fei Yu, and Fei Ma. Enhancing long video question answering with scene-localized frame grouping. *arXiv preprint arXiv:2508.03009*, 2025. 2
- [47] Shoubin Yu, Jaemin Cho, Prateek Yadav, and Mohit Bansal. Self-chained image-language model for video localization and question answering. *Advances in Neural Information Processing Systems*, 36:76749–76771, 2023. 7